

Coloring of DT-MRI Fiber Traces Using Laplacian Eigenmaps

Anders Brun¹, Hae-Jeong Park², Hans Knutsson³, and Carl-Fredrik Westin¹

¹ Laboratory of Mathematics in Imaging, Brigham and Women's Hospital,
Harvard Medical School, Boston, USA,
{anders,westin}@bwh.harvard.edu

² Clinical Neuroscience Div., Lab. of Neuroscience,
Boston VA Health Care System-Brockton Division,
Dep. of Psychiatry, Harvard Medical School
and Surgical Planning Laboratory,
Brigham and Women's Hospital, Harvard Medical School,
hjpark@bwh.harvard.edu

³ Medical Informatics, Linköping University,
Inst. för medicinsk teknik, Universitetssjukhuset,
Linköping, Sweden
knutte@imt.liu.se

Abstract. We propose a novel post processing method for visualization of fiber traces from DT-MRI data. Using a recently proposed non-linear dimensionality reduction technique, Laplacian eigenmaps [3], we create a mapping from a set of fiber traces to a low dimensional Euclidean space. Laplacian eigenmaps constructs this mapping so that similar traces are mapped to similar points, given a custom made pairwise similarity measure for fiber traces. We demonstrate that when the low-dimensional space is the RGB color space, this can be used to visualize fiber traces in a way which enhances the perception of fiber bundles and connectivity in the human brain.

1 Introduction

Diffusion Tensor MRI (DT-MRI) makes it possible to non-invasively measure water diffusion, in any direction, deep inside tissue. In fibrous tissue such as muscles and human brain white matter, water tend to diffuse less in the directions perpendicular to the fiber structure. This means that despite the fact that spatial resolution in MRI is too low to identify individual muscle fibers or axons, a macroscopic measure of diffusion in a voxel may still reveal information about the fiber structure in it. Using DT-MRI it is therefore possible to infer the direction of the fiber in for instance white matter in the human brain. In particular, it is possible to estimate the direction of the fibers when the fiber organization is coherent within the voxel.

When a whole volume of data is acquired using DT-MRI, each voxel contains information about the local characteristics of diffusion inside that particular voxel. The diffusion is described by a tensor D , a symmetric positive definite 3×3 matrix, which

through the Stejskal-Tanner equation (1) explains the measurements obtained from the MR scanner

$$S_k = S_0 e^{-b \hat{g}_k^T D \hat{g}_k}. \quad (1)$$

Here \hat{g}_k is a normalized vector describing the direction of the diffusion-sensitizing pulse, b is the diffusion weighting factor [11] and S_0 is a non-diffusion weighted measure. In order to estimate a tensor D inside each voxel, at least one non-diffusion weighted image S_0 and six diffusion weighted images with different directions are needed [18]. The product $\hat{g}_k^T D \hat{g}_k$ is often referred to as the Apparent Diffusion Coefficient, ADC, and describes the amount of diffusion in the gradient direction.

The tensor can be visualized as an ellipsoid, described by the eigenvectors of the diffusion tensor D , scaled with the square root of their respective eigenvalue. This ellipsoid will represent an isosurface of the probability distribution which describes the position of a water molecule, due to diffusion, a short time after it has been placed in the center of the tensor. A spherical ellipsoid therefore corresponds to an isotropic tensor, which describes that water diffusion is equally probable in any direction. When the ellipsoid is more oblate or elongated, it means that water diffuses less or more in a particular direction, and the tensor is therefore referred to as anisotropic. The anisotropy is often characterized using some rotationally invariant and normalized tensor shape measure, for instance the Fractional Anisotropy index [18]

$$FA = \frac{1}{\sqrt{2}} \frac{\sqrt{(\lambda_1 - \lambda_2)^2 + (\lambda_2 - \lambda_3)^2 + (\lambda_1 - \lambda_3)^2}}{\sqrt{\lambda_1^2 + \lambda_2^2 + \lambda_3^2}}. \quad (2)$$

One of the most intriguing uses of DT-MRI data is the possibility to follow and visualize fiber pathways in the brain. Traditionally this has been accomplished using fiber tracking algorithms, see for instance [1,2,18]. In these approaches a path originating from a seed point is calculated by iteratively moving a virtual particle in the direction in which diffusion is strongest, the principal diffusion direction (PDD). This direction corresponds to the major eigenvector of the diffusion tensor, which is the eigenvector corresponding to the largest eigenvalue. It is widely believed that for human brain white matter, in areas where the diffusion tensors are highly anisotropic, the PDD is highly correlated with the orientation of the underlying fiber structure.

One way to visualize the fiber organization of white matter is to place a virtual particle inside a voxel in white matter and iteratively move it according to a velocity field defined by the principal diffusion direction. This trace will be aligned with the underlying fiber structures and visualizing it will give the impression of looking at actual fiber pathways.

This paper will in the following sections introduce a novel post processing method for visualization of fiber traces from DT-MRI. We will focus on enhancing the perception of organization and connectivity in the data. The method will not specifically address the shortcomings of fiber tracking, but assume that a set of fiber traces has already been obtained. Instead the main contribution of this paper will be to show how a spectral non-linear dimensionality reduction technique, such as Laplacian eigenmaps, can be applied to the problem of organizing fiber trace data. The main application will be visualization of large collections of fiber traces.

2 Previous Work

Visualization of DT-MRI still poses a challenge for the medical imaging community, since the data is high dimensional and contains a lot of interesting anatomical structure. A simple but effective way to visualize tensor data is to map the tensors to scalars or colors and then visualize the data using any method for volume or image visualization. Commonly used scalar mappings include Fractional Anisotropy Index, trace and the norm of the tensor. Color mapping has also been used to encode orientation of the PDD. While these mappings are good in some applications, they are unintuitive or insufficient in others.

To cope with the high dimensionality of tensor data, special tensor glyphs have been designed, see for instance [18]. Commonly used glyphs are short line segments showing the orientation of the PDD and ellipsoids representing all six degrees of freedom of a tensor. Other interesting approaches to encode tensor shape and orientation are reaction diffusion patterns [10] and line integral convolution [12].

Fiber traces, as described in the introduction, have been successfully used to reveal fiber pathways in the brain, see for instance [2]. Often the traces have been represented by streamtubes [19], sometimes in combination with coloring schemes and/or variation of the streamtube thickness according to some quality of the underlying tensor field.

In the area of post processing of fiber traces, prior to visualization, work on clustering of fiber traces have been reported recently. These approaches depend on a similarity measure between pairs of fiber traces, which is used in combination with a traditional clustering method (“fuzzy c-means clustering” [15] and “K nearest neighbors” [6]). Outside the medical field, model based curve clustering has been studied in [8]. The method presented in this article will share many similarities with automatic clustering methods. It will however give a continuous coloring of the fiber traces, as opposed to the discrete set of labels assigned during clustering. It could also be considered as a preprocessing step to clustering. Similar to the clustering methods, our approach is automatic and involves no user intervention except parameter selection. This is in sharp contrast from manual approaches to organize traces into bundles, such as the virtual dissection proposed in [5]. However, all the post processing methods for fiber traces share the same weakness: they rely on a good fiber tracking algorithm to perform well.

3 Embedding Fiber Traces – A Motivation

If fiber traces are initiated from seed points in the entire white matter, as in figure 1 left, a quick glance motivates the need for some kind of color mapping in order to enhance the perception of the fiber organization in the brain. We therefore propose a post processing step, prior to visualization, in which each fiber trace is assigned a color from a continuous RGB color space. The intuition is that similar traces should be assigned similar colors, while dissimilar traces are mapped to dissimilar colors. This will enhance the visualization of fiber bundles.

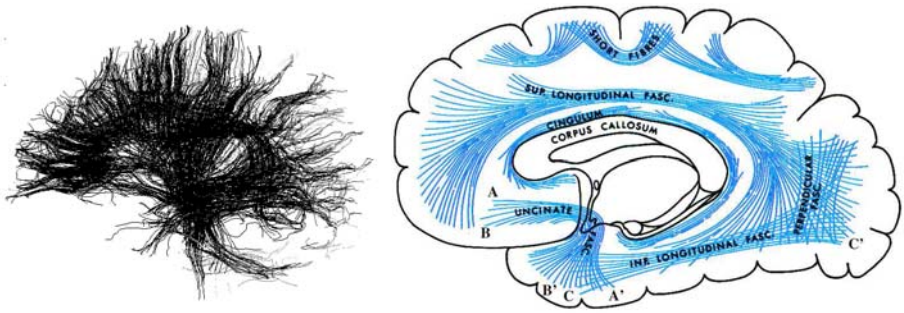


Fig. 1. Left: Fiber traces from a human brain. Simple PDD fiber tracking have been initiated from and constrained to voxels with high anisotropy index. A sagittal view. The head facing left. **Right:** A schematic view of major fiber bundles in the brain. Adapted from Gray's *Anatomy of the Human Body* as displayed at Bartleby.com.

4 Spectral Clustering and Embedding

In order to map the fiber traces we use a spectral embedding technique called Laplacian eigenmaps which was recently proposed by Belkin and Niyogi in [3]. The core of the algorithm is the use of a local similarity measure, which is used to construct a graph in which each node correspond to a data point and where the edges represent connections to neighboring data points. It is the structure of this graph which represents the manifold to be discovered, which is accomplished through the solution of an eigenvalue problem which maps each data point to a low-dimensional Euclidean space. This mapping locally preserves the graph structure. In short, points close in the graph are mapped to nearby points in the new Euclidean space.

In our application, the data points are fiber traces. The effect we would like to obtain is that traces within a fiber bundle are mapped to similar points in the low-dimensional space. The manifolds we hope to reveal would correspond to a parameterization of a specific fiber bundle. Not a parameterization along the fibers – all points of a fiber trace should project to the same point in the new low-dimensional space – but in the direction perpendicular to the fibers. In the case of a thin bundle such as the cingulate fasciculus we would expect a clustering effect to dominate, all traces within this thin bundle should project to more or less a single point in a low dimensional space. On the other hand, a large bundle structure such as the corpus callosum can be parameterized along the anterior-posterior axis and we would expect it to be represented as a one-dimensional manifold.

While fiber traces naturally reside in a low dimensional 3-D space, a trace itself must be considered as a high-dimensional object, or at least an object which we have difficulties in representing as a point in a low dimensional vector space. Constructing an explicit global similarity measure for fiber traces is also somewhat difficult – to what extent are two traces similar? How can we come up with a similarity measure which corresponds to a mapping of traces into a low-dimensional space? Luckily Laplacian eigenmaps and other spectral methods only needs a local similarity measure, a measure

which determine the similarity between a data point and its neighbors. This means that we only need to construct a similarity measure which is able to identify and measure similarity between two very similar traces. In the case of two very dissimilar traces, we may assume zero similarity.

Using this similarity measure, a graph is constructed in which nodes represent fiber traces and where edges connect neighboring traces.

5 Laplacian Eigenmaps

For an in depth explanation of Laplacian eigenmaps, as explained by Belkin and Niyogi, see [3]. In brief, the algorithm for Laplacian eigenmaps consists of three steps:

1. Construction of a graph where each node corresponds to a data point. Edges are created between nodes which are close to each other in the original space. A neighborhood of fixed size around each data point or the set of K nearest neighbors could for instance be used as criteria for creating the edges in the graph.
2. Weights are assigned to each edge in the graph. In general, larger weights are used for edges between points which are close to each other in the original space. In the simplest case, all weights are set to 1. A Gaussian kernel or similar could also be used.
3. Solution of the generalized eigenvalue problem:

$$D_{ij} = \begin{cases} \sum_{k=1}^N W_{ik} & \text{if } i = j \\ 0 & \text{if } i \neq j \end{cases} \quad (3)$$

$$L = D - W \quad (4)$$

$$Ly = \lambda Dy \quad (5)$$

where N is the number of nodes and L is called the Laplacian matrix of the graph. The eigenvectors derived from equation 3 are ordered according to their eigenvalues. Due to the structure of the L , the smallest eigenvalue will correspond to a constant eigenvector and is discarded, but the n eigenvectors corresponding to the next smallest eigenvalues are used as embedding coordinates for the data points in the new space.

We never performed the formation of the graph in step one explicitly, but performed a thresholding of the weights so that very small weights were set to zero, which corresponds to absence of an edge in the graph.

Laplacian eigenmaps share many similarities with other recent spectral algorithms for clustering and embedding of data, for instance Kernel PCA [14] and spectral methods for image segmentation [13], and we expect a qualitatively similar behavior from all of them even if the interpretation of the results is somewhat different in the various methods. For a unifying view of the behavior of spectral embeddings and clustering algorithms, see [4]. One of the most important aspects of spectral methods for clustering and embedding, including Laplacian eigenmaps, is the fact that they are all posed as eigenvalue problems, for which efficient algorithms are widely available.

6 Similarity Through Connectivity

There is no similarity measure given for fiber traces per se and therefore many ways of choosing the edge weights exist. In this initial effort to cluster and embed traces for visualization purposes, we will only try a simple but yet effective similarity measure.

The measure is based on the idea that two traces with similar end points should be considered similar. That is, we only look at the endpoints for a pair of fiber traces, and discard all other information. In figure 1 (right) we would for instance want a trace with endpoints $\{A,A'\}$ to have high similarity with a trace with endpoints $\{B,B'\}$. However, trace $\{C,C'\}$ should be considered dissimilar from both $\{A,A'\}$ and $\{B,B'\}$, even though they all share a common origin. This could also be interpreted as a measure of connectivity.

Here $f_{i,1}$ and $f_{i,\text{end}}$ corresponds to the first and last coordinates of the i th fiber trace and W_{ij} is the weight between nodes / fiber traces i and j :

$$f_i = (f_{i,1}, f_{i,\text{end}}), \quad (6)$$

$$\tilde{f}_i = (f_{i,\text{end}}, f_{i,1}), \quad (7)$$

$$W_{ij} = \begin{cases} 0 & \text{if } i = j \\ \exp\left(-\frac{\|f_i - f_j\|^2}{2\sigma^2}\right) + \exp\left(-\frac{\|f_i - \tilde{f}_j\|^2}{2\sigma^2}\right) & \text{if } i \neq j \end{cases} \quad (8)$$

We note that W_{ij} is symmetric with respect to i and j . This measure is also invariant to re-parameterization of the fiber trace, for instance reverse numbering the fiber trace coordinates. It will also give traces which connects similar points in space a large weight while dissimilar connectivity will result in a weight close to zero given that σ is chosen carefully.

This similarity measure will work fine in most cases where the fiber traces are not damaged and really connect different parts of the brain in an anatomically correct way. Other similarity measures used in clustering methods have been based on correlation measures between fiber traces [15,6]. Those correlation measures could be used as well to build up the graph needed by a spectral embedding method such as Laplacian eigenmaps. For the purpose of demonstration and under the assumption that the fiber traces are ok, the above described similarity should work fine and it is also faster to compute than correlation measures.

7 In vivo DT-MRI Data

Real DT-MRI data from the brain of a healthy volunteer was obtained at the Brigham and Women's Hospital using LSDI technique on a GE Signa 1.5 Tesla Horizon Echospeed 5.6 system with standard 2.2 Gauss/cm field gradients. The time required for acquisition of the diffusion tensor data for one slice was 1 min; no averaging was performed. The voxel resolution was $0.85\text{mm} \times 0.85\text{mm} \times 5\text{mm}$.

A random sample of 4000 points inside white matter with diffusion tensors having high FA were selected as seed points for the fiber tracking. Traces were then created by tracking in both directions starting from these seed points, following the principal eigenvector of diffusion using a step length of 0.5mm and linear interpolation of the

tensors. The tracking was stopped when reaching a voxel with FA lower than certain threshold approximately corresponding to the boundary between white and gray matter. Fiber traces shorter than 10mm were removed. This resulted in a set of approximately 3000 fiber traces.

8 Experiments

The algorithm was implemented in Matlab. While the number of fiber traces were at most 5000 the PDD tracking method, calculation of the graph Laplacian and the solution of the generalized eigenvalue problem could be performed without optimizations. Matlab was used for visualization except in figure 5, where the in-house software 3-D Slicer [9] was used.

For the color mapping, the The second, third and fourth eigenvector were scaled to fit into the interval $[0, 1]$ and then used for the channels red, green and blue, to color the corresponding fiber traces.

The embedding of fiber traces into a RGB color space was tested first on synthetic data, then on real human brain DT-MRI data. The synthetic toy examples should be considered as illustrations of the method rather than near realistic or challenging experiments.

Figure 2 shows how the embedding into color space works for a set of fiber traces arranged as a Möbius strip. The traces on (left) are mapped into an RGB space, which determines the color of each trace. In the right plots, the image of this mapping in RG space (first two embedding coordinates) is shown. Each dot in the right plots correspond to a single trace in the left plots. The circular structure of the Möbius strip can thus be seen in the geometry of the left image, in the coloring of the left image and in the shape of the fiber bundle after embedding it into RG space to the right.

Figure 3 (left) shows how traces connecting opposite sides of a sphere are colored. Coloring according to the three first embedding coordinates. This set of traces has the topology of the “projective plane”, P_2 . Note that even though it is impossible to see the traces inside the sphere, we can deduce how traces connect by looking at the colors which match on opposite sides. However, the projective plane cannot be embedded in three dimensions without intersecting itself, which means that the color mapping of this set of traces is many-to-one in some sense.

Figure 3 (right) shows a synthetic example of four fiber bundles, two crossing each other and two having the same origin. Because of our similarity measure based on connectivity of the fiber trace endpoints, crossings and overlaps will not disturb the embedding. Laplacian eigenmaps will color each in a color close to its neighbors colors. In this case the clustering properties of Laplacian eigenmaps becomes obvious, which is welcomed as no obvious manifold structure exists in the data.

The experiments on real data in figures 4 and 5 show how the method works in practice. The value of the only parameter σ was chosen empirically. Starting with a large sigma is safe in general, while a too small sigma give unstable solutions of the eigenvalue problem. In figure 5 an example is shown where the fiber traces have been projected back to a T2 weighted coronal slice.

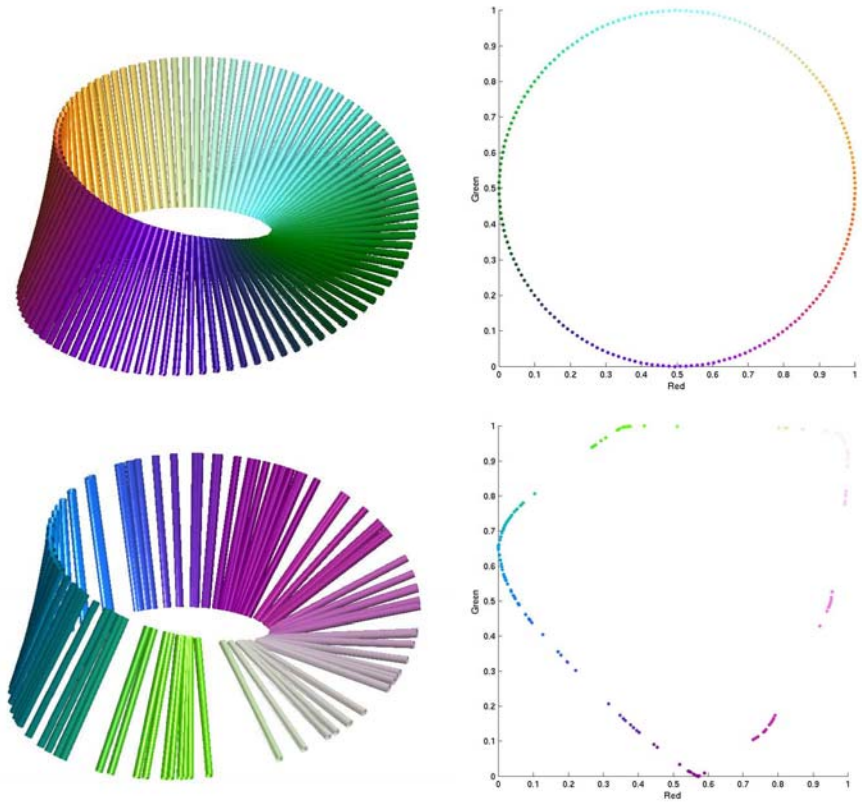


Fig. 2. Synthetic toy examples of coloring “fiber traces” shaped as a Möbius strip. **Top:** A very regular bundle (left) and its embedding (right). Note how the embedding finds a perfect circle. **Bottom:** A more random bundle (left) and its embedding using a little too small σ (right). Note how the embedding tends to enhance clusters in the data, but the topology is still somewhat a circle.

9 Discussion

All the figures show different aspects of the idea of using Laplacian eigenmaps, together with a custom made similarity measure, to enhance the visualization of fiber organization. Both the synthetic and real brain data show very promising results, and the colors reveal that the method has been able to organize and embed the fiber traces into a space where different anatomical structures have been mapped to different positions. In the real brain data, it can for instance be noted that traces on the left hemisphere in general have a different color from those on the right. Small structures such as the cingulum, going from posterior to anterior above the corpus callosum, are also more visible thanks to the coloring.

The experiments presented in this paper have been chosen with great care. Finding the correct σ has not always been easy and what is a good embedding of fiber traces in



Fig. 3. Synthetic examples with “fiber traces” connecting opposite points on a sphere (left) and with four fiber bundles (right), two crossing each other and two having the same origin. Coloring according to the three first embedding coordinates.

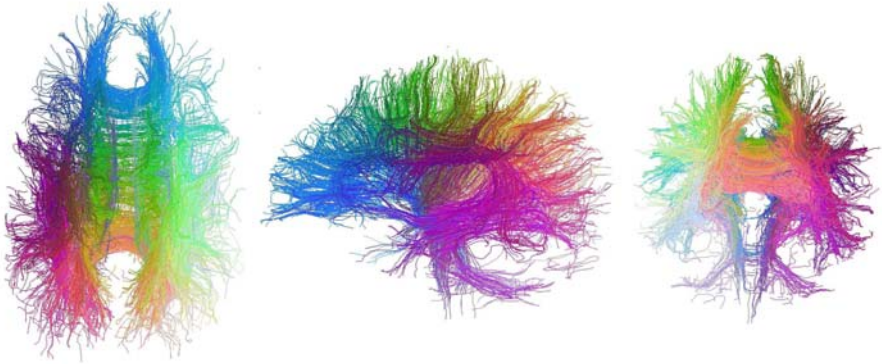


Fig. 4. Fiber traces from a human brain, colored such that traces with similar endpoints have been assigned similar colors. Simple PDD fiber tracking have been initiated from and constrained to voxels with high anisotropy index. **Left:** Axial view. The head facing up. **Middle:** Sagittal view. The head facing left. **Right:** Coronal view. The head facing inwards.

RGB-space for visualization is subjective. Optimal choice of σ as well as an analysis of the stability for the embedding is certainly interesting topics for future research.

We have so far not focused on optimizing the speed of this post processing method for fiber traces. After the coloring is only done once per dataset. However, for more than a maximum of 5000 fiber traces used in our experiments, we feel there is a need to take greater care in terms of memory management and speed. First of all the eigenvalue problem solved in Laplacian eigenmaps is sparse, given the right similarity measure.

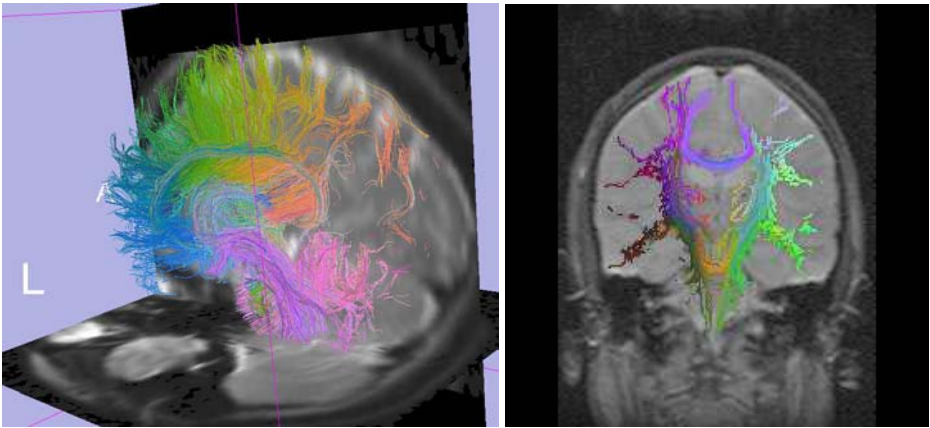


Fig. 5. Left: Fiber traces from a human brain, colored such that traces with similar endpoints are assigned similar colors. A cutting plane is used to give a cross section view of corpus callosum and slices from a T2 weighted volume add additional understanding of the anatomy. Visualization done using the 3-D Slicer [9]. **Right:** Fiber traces from a human brain, colored such that traces with similar endpoints are assigned similar colors. Only the intersection of the traces with a coronal T2 weighted slice is shown. This kind of voxel coloring could for instance assist when manually segmenting white matter in DT-MRI images.

Also there exists methods to reduce the size of the eigenvector calculation by using sampling methods such as in the Nyström method [7].

The similarity measure used so far is efficient, but simple. Correlation measures of fiber trace similarity have been used by other groups and this method for fiber trace visualization could definitely benefit from a better definition of local fiber trace similarity. Two issues raises. One is to define a better similarity measure which is able to “glue together” broken fiber traces, as fiber tracking is sensitive to noise. The other issue is speed, as the fiber trace similarity measure is evaluated for all pairs of traces. We have done experiments with highly efficient and more correlation-like similarity measures, but the results are still too preliminary to present here.

10 Conclusion

The goal of this project was to find a post processing method for DT-MRI fiber traces, to enhance the perception of fiber bundles and connectivity in the brain in general. We can conclude that despite the simplicity of the similarity function, this approach based on Laplacian eigenmaps has been able to generate anatomically interesting visualizations of the human brain white matter. Many interesting new topics arise in the light of this novel way of organizing DT-MRI data: clustering, segmentation and registration being prominent candidates for future research.

Acknowledgments. Thanks to Martha Shenton, Ron Kikinis, Stephan Maier, Steve Haker, Eric Pichon, Jonathan Sacks and Mats Björnemo for interesting discussions.

This work was funded in part by NIH grants P41-RR13218 and R01 MH 50747, and CIMIT. It was also supported in part by the Post-doctoral Fellowship Program of Korea Science & Engineering Foundation (KOSEF).

References

1. P. J. Basser Inferring microstructural features and the physiological state of tissues from diffusion-weighted images. *NMR in Biomedicine*. 8 (1995) 333–344.
2. P. J. Basser, S. Pajevic, C. Pierpaoli, J. Duda, and A. Aldroubi In vivo fiber tractography using DT-MRI data. *Magn. Reson. Med.* 44 (2000) 625–632.
3. M. Belkin and P. Niyogi Laplacian eigenmaps and spectral techniques for embedding and clustering. in T. G. Diettrich, S. Becker, and Z. Ghahramani (eds:) *Advances in Neural Information Processing Systems 14*. MIT Press, Cambridge, MA 2002.
4. M. Brand and K. Huang A unifying theorem for spectral embedding and clustering. 2003.
5. M. Catani, R. J. Howard, S. Pajevic, and D. K. Jones. Virtual in vivo interactive dissection of white matter fasciculi in the human brain. *Neuroimage* 17, pp 77–94, 2002.
6. Z. Ding, J. C. Gore, and A. W. Anderson. Classification and quantification of neuronal fiber pathways using diffusion tensor MRI. *Mag. Reson. Med.* 49:716–721, 2003.
7. C. Fowlkes, S. Belongie, and J. Malik. Efficient Spatiotemporal Grouping Using the Nyström Method *CVPR*, Hawaii, December 2001.
8. S. J. Gaffney and P. Smyth. Curve clustering with random effects regression mixtures. in C. M. Bishop and B. J. Frey (eds:) *Proc. Ninth Int. Workshop on AI and Stat.*, Florida, 2003.
9. D. Gering, A. Nabavi, R. Kikinis, W. Eric L. Grimson, N. Hata, P. Everett, F. Jolesz, and W. Wells III. An Integrated Visualization System for Surgical Planning and Guidance using Image Fusion and Interventional Imaging. *Proceedings of Second International Conference on Medical Image Computing and Computer-assisted Interventions, Lecture Notes in Computer Science*, pp. 809–819, 1999.
10. G. Kindlmann, D. Weinstein, and D. Hart Strategies for Direct Volume Rendering of Diffusion Tensor Fields *IEEE transactions on Visualization and Computer Graphics* Vol. 6, No. 2. 2000.
11. D. Lebihan, E. Breton, D. Lallemand, P. Grenier, E. Cabanis, and M. LavalJeantet MR imaging of intravoxel incoherent motions: application to diffusion and perfusion in neurologic disorders. *Radiology* 161, 401–407, 1986.
12. T. McGraw, B. C. Vemuri, Z. Wang, Y. Chen, and T. Mareci Line integral convolution for visualization of fiber tract maps from DTI *Proceedings of Fifth International Conference on Medical Image Computing and Computer-assisted Interventions*, Lecture Notes in Computer Science, pp. 615–622, 2003.
13. M. Meila and J. Shi A random walks view of spectral segmentation. In *AI and Statistics (AISTATS) 2001*, 2001.
14. B. Schölkopf, A. Smola, and K. Müller Nonlinear component analysis as a kernel eigenvalue problem. *Neural Computation*, 10(5):1299–1319, 1998.
15. J. S. Shimony, A. Z. Snyder, N. Lori, and T. E. Conturo Automated fuzzy clustering of neuronal pathways in diffusion tensor tracking. *Proc. Intl. Soc. Mag. Reson. Med.* 10, Honolulu, Hawaii, May 2002.
16. E. Weisstein Eric Weisstein’s world of mathematics. <http://mathworld.wolfram.com/>, May 15, 2003. .
17. C.-F. Westin, S. Peled, H. Gudbjartsson, R. Kikinis, and F. A. Jolesz Geometrical Diffusion Measures for MRI from Tensor Basis Analysis *Proc. of the International Society for Magnetic Resonance Medicine (ISMRM)*, Vancouver Canada, April 1997.

18. C.-F. Westin, S. E. Maier, B. Khidir, P. Everett, F. A. Jolesz, and R. Kikinis. Image Processing for Diffusion Tensor Magnetic Resonance Imaging *Proceedings of Second International Conference on Medical Image Computing and Computer-assisted Interventions, Lecture Notes in Computer Science*, pp. 641–652, 1999.
19. S. Zhang, T. Curry, D. S. Morris, and D. H. Laidlaw. Streamtubes and streamsurfaces for visualizing diffusion tensor MRI volume images. *Visualization '00 Work in Progress* October 2000.